Mapping the subsurface resistivity using geostatistics

Jerbeson M. Santana (PPGG/UFRN) and Walter E. Medeiros (DGEF/UFRN & INCT-GP)

This paper was prepared for presentation at the 14th International Congress of the Brazilian Geophysical Society, held in Rio de Janeiro, Brazil, August 3-6 2015.

Abstract

It is presented a new method for the approximate mapping of the subsurface resistivity based on a geostatistical approach. It are used the characteristic points (CPs) of a resistivity sounding, which are their inflection and extreme (maximum and minimum) points. The methodology consists of four stages: i) smoothing the geoelectric soundings to assure robusteness to measurement errors, ii) determining the CPs from the smoothed versions of the geoelectric soundings, and obtaining from the CPs point estimates for the subsurface resistivity using empirical relations between electrode spacing and depth, iii) calculating semivariograms associated to the point estimates, and fitting them to a semivariogram model, and finally iv) estimating the subsurface resistivity distribution by kriging interpolation of the point estimates. The method's performance is demonstrated with real 2D Schlumberger array data.

Introduction

Geostatistics has long been applied to geophysical problems. For geoelectrical methods, examples of application include quantifying the spatial correlation between apparent resistivity data to improve geological interpretations of sparse data over large areas (Joëlle et al., 2011), estimating narrower intervals for model parameters to reduce ambiguities in quantitative interpretations (Kumar et al., 2007), obtaining improved correlations between geoelectrical and hydrogeological parameters in order to characterize aquifers (e.g. Yang and Lee, 2002; Sainato and Losinno, 2006; Slater, 2007), estimating physical properties of soil from electrical conductivity based on multivariate geostatistical analysis (Morari et al., 2009), evaluating the resolution of resistivity tomograms (Day-Lewis et al., 2005), and establishing theoretical basis for inversion approaches (Yeh et al., 2002).

Here it is presented a method for the approximate mapping of the subsurface resistivity based on a geostatistical treatment of the characteristic points of a resistivity sounding. These points are the inflection and extreme (maximum and minimum) points. In this new combination of these two old elements (classic geostatistics and characteristic points) no assumptions are made about the subsurface resistivity distribution and, as result, the method is robust to the model dimension. In addition, the method is also robust to measurement errors and computationally very fast because no modeling (either direct or inverse) is demanded. Given its robustness, it can be readily implemented as a fast automatic method of interpretation.

Methodology

The present approach is based on the use of the characteristic points (CPs) of geoelectric soundings to compose a regionalized variable for geostatistical treatment. The methodology consists of four simple stages: i) smoothing the geoelectric soundings to assure robusteness to error content, ii) determining the CPs from the smoothed version of the geoelectric soundings and obtaining from these CPs point (or punctual) estimates for the subsurface resistivity, iii) calculating semivariograms associated to the point estimates and fitting them to semivariogram models, and iv) estimating the subsurface resistivity distribution by kriging interpolation of the point estimates. In the present implementation, it are used DC-resistivity Schlumberger array soundings arranged as 2D data along a distance y. For convenience, the apparent resistivity data ρ_a is plotted as function of electrode spacing $AB/4$.

Characteristisc points - CPs

The CPs of a geoelectric sounding are their inflection and extreme (maximum and minimum) points (Figure 1). Given a geoelectric sounding at position y on the Earth's surface, point estimates for the subsurface resistivity distribution $\rho(y,d)$ at depth d can be obtained by using the pairs of $AB/4$ and ρ_a associated with the CPs. Taking the schematic sounding in Figure 1 as example, it are identified five CPs (I to V). In the following, the electrode spacing $AB/4$ is used as an approximate estimate of depth, as is conventional for the case of the Schlumberger array. Using this empirical relation, three point estimates $\rho(y,d)$ can be obtained (Figure 1): $\rho(y,\frac{1}{4}AB_{(II)}) = \rho_{a(I)}$, $\rho(y,\frac{1}{4}AB_{(IV)}) = \rho_{a(III)}$, and $\rho(y,\frac{1}{4}AB_{(V)}) = \rho_{a(V)}$. Note that a point estimate is usually obtained by attributing the resistivity value of an extremum to the electrode spacing of the previous inflection point, except for the last point estimate. The possible additional point estimate $\rho(y,\frac{1}{4}AB_{(I)}) = \rho_{a(I)}$ is discarded because it is a redundant point from the geostatistical viewpoint. Note also that if the subsurface were interpreted with the 1D layer-cake model, it would be possible to compose a first estimate of thickness and resistivity for the layers using the point estimates. In the following, it is used the notation $\rho(y,\widehat{\frac{AB}{4}}) = \widehat{\rho_a}$ to identify a generic subsurface point resistivity estimate obtained from the CPs.

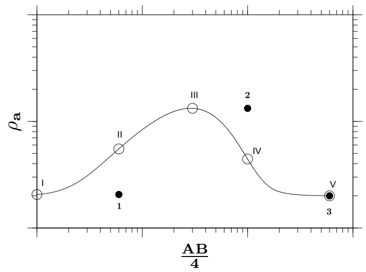

Point estimate	Depth	Resistivity
1	$\frac{1}{4}AB_{(II)}$	$\rho_{a(I)}$
2	$\frac{1}{4}AB_{(IV)}$	$\rho_{a(III)}$
3	$\frac{1}{4}AB_{(V)}$	$\rho_{a(V)}$

Figure 1: Schematic Schlumberger sounding and its characteristic points - CPs (open circles) marked from I to V. Black dots (**1** to **3**) are the point resistivity estimates. The table shows how values of AB/4 spacing are combined with the extreme values of apparent resistivity to compose the point resistivity estimates.

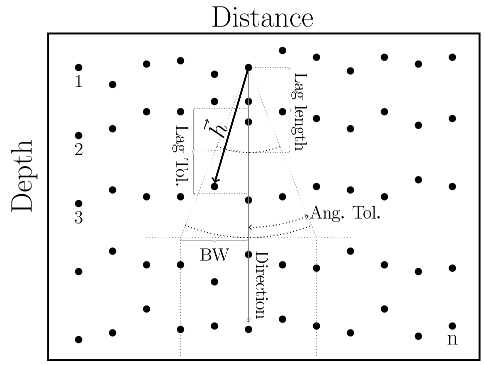

Figure 2: Schematic 2D distribution of point resistivity estimates (black dots) and the search parameters in an irregular mesh. The point resistivity estimates result from the characteristic points (CPs) of the smoothed version of the resistivity soundings and are used as the regionalized variable for the geostatistical approach.

Because real geoelectrical soundings always present irregularly spaced data containing measurement errors, it is necessary to apply a smoothing or interpolating operator before identifying the CPs. That is, to assure robusteness to measurement errors, the CPs are identified from a smoothed version of the soundings. Smooth versions of the resistivity soundings were here obtained by cubic spline interpolation. As result, it is assured continuity both to the first and second derivatives of the smooth version of the soundings. Thus, the extreme and inflection points can then be easily identified as the points where the first and second derivatives, respectively, have null values.

Geostatistics of the characteristisc points

The point estimates $\rho(y, \widehat{\frac{AB}{4}}) = \widehat{\rho}_a$ are ordered from 1 to n (Figure 2). Let $z(\mathbf{X}_i) = \rho_i(y, \widehat{\frac{AB}{4}})$ $(i = 1,2,3...n)$ be the regionalized variable, being $\mathbf{X}_i$ the position vector identifying the i-th subsurface point $(y, \widehat{\frac{AB}{4}})$. Given a direction $\mathbf{h}$ in the plane $(y, \widehat{\frac{AB}{4}})$, the experimental semivariogram can then be calculated (Matheron, 1971):

$$\hat{\gamma}(h) = \frac{1}{2N(h)} \sum_{i=1}^{N(h)} [z(\mathbf{X}_i) - z(\mathbf{X}_i + \mathbf{h})]^2, \qquad (1)$$

where $h = \|\mathbf{h}\|$ is the Euclidean distance between point estimates, and $N(h)$ is the number of pairs of points between observations $z(\mathbf{X}_i)$ and $z(\mathbf{X}_i + \mathbf{h})$. When data are irregularly spaced, as in present case, a search technique must be used to calculate the semivariogram (Matheron, 1971). A search technique is specified by the parameters: lag number, lag length, lag tolerance, lag direction, angular tolerance, and bandwidth (BW), as illustraded in Figure 2. After a series of tests, it was verified that using just the unidirectional semivariogram along depth give the best results.

The experimental semivariogram must be fitted with a semivariogram model, as Gaussian, spherical or exponential (Matheron, 1971), for example. In the casepresented in this study, the spherical model furnished the best least-squares fitting. The spherical model is defined by

$$\begin{aligned} \hat{\gamma}(h) &= C_0 + C\left[\frac{3h}{2a} - \left(\frac{h}{2a}\right)^3\right], \ h < a \\ \hat{\gamma}(h) &= C_0 + C, \ h > a, \end{aligned} \qquad (2)$$

where C_0, C, and a are the nugget effect, still, and range, respectively.

After the semivariogram model parameters are obtained, a kriging interpolation (ordinary or lognormal) is applied for the point resistivity estimates to map approximately the subsurface resistivity distribution.

Application

To show the performance of our methodology, we apply it to real 2D Schlumberger data. To calculate 2D apparent resistivity data it is used the finite-difference modeling approach described by Dey and Morrison (1979). In order to appraise the validity of the subsurface resistivity distribution estimated with the present geostatistical approach, these results are compared with inversion estimates obtained using the smoothness constraint (deGroot Hedlin and Constable, 1990). To quantify the degree of fitting between the apparent resistivity observations r_i and the corresponding generated values g_i (either using geostatistics or inversion), it is used the function:

$$\varepsilon = 100 \sum_i \frac{(g_i - r_i)^2}{r_i^2} \ \%. \qquad (3)$$

Figure 3a shows an apparent resistivity section constructed with 105 measurements using the Schlumberger array (Medeiros, 1987; Medeiros and Lima, 1990). The survey was done by using 21 equally spaced stations, with distance between stations equal to 20 m. In each station, five apparent resistivity values were measured with $AB/2$

= 5, 10, 20, 50, and 100 m. The survey area has flat topography so that its effects in the apparent resistivity data can be neglected. The survey geologic context is an area of crystalline rocks in Bahia state, Brazil, mainly composed by gneiss. The study objective was to appraise criteria for locating boreholes for groundwater production in fracture zones (Medeiros and Lima, 1990). As a general guide, boreholes are located in zones where the crystalline rock is intensively fractured and/or altered by weathering, thus generating favorable conditions for groundwater storage. Usually these zones appear in apparent resistivity sections as relatively large and deep conductive anomalies, like the anomaly seen between positions 200 m and 300 m (Figure 3a). From the quantitative point of view, the interpretation objectives are to estimate the depth to the fresh rock and to separate shallow conductive materials, like clay soil, from the fractured and/or weathered rock, because these two effects are generally superposed. In fact, in the apparent resistivity section these two effects can hardly be separated in the position interval 200 m - 300 m (Figure 3a). Using the CPs, 53 irregularly spaced

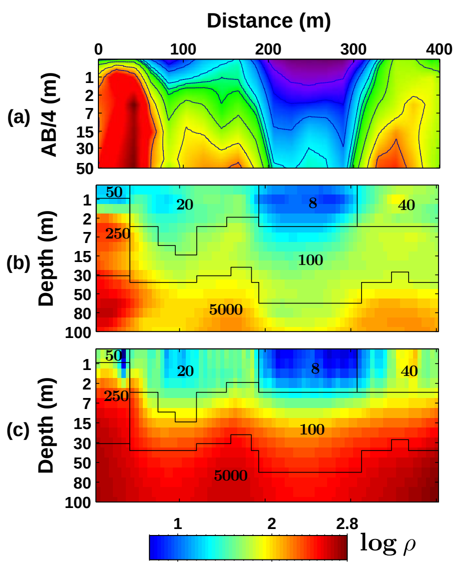

Figure 3: (a) observed apparent resistivity section, (b) resistivity distribution obtained with geostatistics, and (c) inversion result incorporating the smoothness constraint (deGroot Hedlin and Constable, 1990). In (b) and (c) it is superposed, as thin black lines and numbers (resistivities in Ωm), a layer model incorporating variations both in thickness and resistivity (Medeiros and Lima, 1990). The colour bar is in decimal logarithm.

point resistivity estimates were obtained. Their coefficient of variation is equal to 1.1, justifying the lognormal transformation (Koch and Link, 2002). A search technique was implemented using the parameters given in the Table 1. The obtained experimental semivariogram is shown in Figure 4. The least-squares fitting of the spherical model to this experimental data gives a root-mean-square equal to 1.3. A lognormal kriging interpolation was performed resulting in the the resistivity distribution obtained with geostatistics (R-G distribution, for short) shown in Figure 3b.

In the position interval 200 m - 300 m, the R-G

Table 1: Parameters used in the search technique to calculate the semivariogram of the irregularly spaced point resistivity estimates in the real data example.

Lag number	Lag length	Lag tol.	Lag dir.	Angular tol.	BW
17	4	2	Vert.	45	12

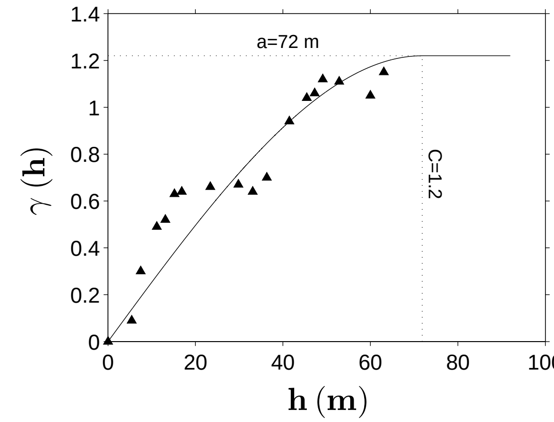

Figure 4: Semivariogram (black triangles) of the point resistivity estimates and its fitting with the spherical model. The still is not defined in the experimental semivariogram due to dispersion and/or lack of data. Then, it is used the lowest possible still in the spherical model.

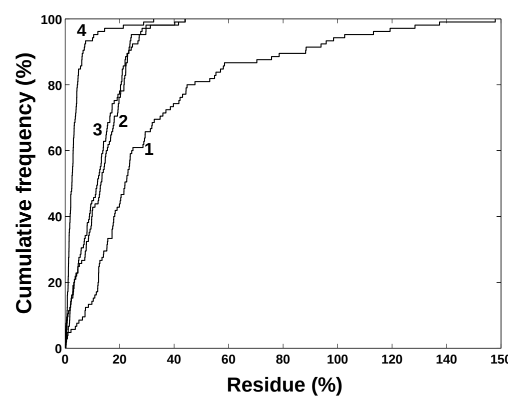

Figure 5: Cumulative frequency curves of the fittings between observed and modeled apparent resistivity data (Equation 3) obtained with four model cases (**1** to **4**). Curves **1**, **2**, and **4**: initial model, 5-th iteration, and 15-th iteration, respectively, of the resistivity estimates obtained with the inversion approach using as initial model the homogeneous semispace. Curve **3**: resistivity distribution resulted from geostatistics. Curve **4** also represents the coincident results of the 9-th iteration of the resistivity estimates obtained with the inversion approach but using as initial model the distribution resulted from geostatistics.

distribution fairly well discriminates the shallow relatively high conductive anomaly, which might be attributed to clay soil, from the intermediate conductive values, which might be attributed to fractured and/or weathered crystalline rock. For comparison, it is superposed the interpretation done by Medeiros and Lima (1990) by using a layer model incorporating variations both in thickness and resistivity. This interpretation was done by a trial-and-error approach (Medeiros, 1987) using a 2D modeling algorithm (Dey and Morrison, 1979), and incorporating geologic information both on soil thickness and depth to the fresh rock avaliable from a borehole located near position 200 m. For an additional comparison, it is also shown in Figure 3c the inversion result obtained with the method of deGroot Hedlin and Constable (1990). The input model for the inversion was a homogeneous semispace with resistivity equal to 130Ωm which is the arithmetic mean of the apparent resistivity data. It seems that the inversion estimate was more affected by the influence of the shallow conductive anomaly than the R-G distribution. As result, the discrepancies in the depth to the fresh rock (assumed to occur around the isovalue curve of 100Ωm) were minimized, in this way causing a lack of relevant information for the geophysical/hydrogeological interpretation. A possible reason to this fact is that the inversion result suffered a higher influence of the longitudinal conductance equivalence than the R-G distribution, because in the latter the thicknesses are tied to the AB/4 spacing.

The Figure 5 it are compared the cumulative frequency distribution curves associated to the fittings between apparent resistivity data (Equation 3) in four cases. In particular, curve 3 shows that the R-G distribution generates apparent resistivity data fitting around 75% of the data within 20%. Thus, as well as in the synthetic data example, the R-G distribution can be considered as a quasi-solution. Another factor contributing to validate this statement is the fact that the layer model allows a global fitting of about 16% (Medeiros and Lima, 1990). Also as in the synthetic data example, starting the inversion algorithm with the R-G distribution allows a faster convergence saving around 40% of the iterations.

Conclusion

It is presented a new method for the approximate mapping of the subsurface resistivity based on a new combination of two old elements: classic geostatistics and characteristic points of a resistivity sounding. No explicit assumptions are made about the true subsurface resistivity distribution and, as result, the method is robust to the model dimension and can be readily implemented for 3D or even 4D data. Computationally, the method is very fast because no modeling is demanded and the most intensive computer operation is just a kriging interpolation. Given its robustness to the model dimension and measurement errors, it can be readily implemented as a fast automatic method of interpretation. The estimated resistivity distribution has value both as an object to interpret and as a better initial model for inversion algorithms. The proposed method might be generalized for other DC-resistivity arrays and electromagnetic techniques based on resistivity soundings.

References

Day-Lewis, F. D., K. Singha, and A. M. Binley, 2005, Applying petrophysical models to radar travel time and electrical resistivity tomograms: Resolution-dependent limitations: Journal of Geophysical Research: Solid Earth, **110**, B08206.

deGroot Hedlin, C., and S. C. Constable, 1990, Occam's inversion to generate smooth, two-dimensional models from magnetotelluric data: Geophysics, **55**, 1613–1624.

Dey, A., and H. Morrison, 1979, Resistivity modelling for arbitrarily shaped two-dimensional structures: Geophysical Prospecting, **27**, 106–136.

Joëlle, R., J. L. Fernández-Martínez, C. Sirieix, O. Harmouzi, A. Marache, and A. Essahlaoui, 2011, A methodology for converting traditional vertical electrical soundings into 2D resistivity models: Application to the Saïss basin, Morocco: Geophysics, **76**, B225–B236.

Koch, G. S., and R. F. Link, 2002, Statistical analysis of geological data: Courier Corporation.

Kumar, D., S. Ahmed, N. S. Krishnamurthy, and B. Dewandel, 2007, Reducing ambiguities in vertical electrical sounding interpretations: A geostatistical application: Journal of Applied Geophysics, **62**, 16–32.

Matheron, G., 1971, The theory of regionalized variables and its applications: École National Supérieure des Mines.

Medeiros, W. E., 1987, The resistivity method applied to the hydrogeology of crystalline terrains: A problem of two-dimensional modelling: Master's thesis, Universidade Federal da Bahia, Brazil, 1987. (in Portuguese).

Medeiros, W. E., and O. A. Lima, 1990, A geoelectrical investigation for ground water in crystalline terrains of central Bahia, Brazil: Groundwater, **28**, 518–523.

Morari, F., A. Castrignanò, and C. Pagliarin, 2009, Application of multivariate geostatistics in delineating management zones within a gravelly vineyard using geo-electrical sensors: Computers and Electronics in Agriculture, **68**, 97–107.

Sainato, C. M., and B. N. Losinno, 2006, Spatial distribution of groundwater salinity at Pergamino: arrecifes zone (Buenos Aires Province, Argentina): Brazilian Journal of Geophysics, **24**, 307–318.

Slater, L., 2007, Near surface electrical characterization of hydraulic conductivity: From petrophysical properties to aquifer geometries—A review: Surveys in Geophysics, **28**, 169–197.

Yang, C.-H., and W.-F. Lee, 2002, Using direct current resistivity sounding and geostatistics to aid in hydrogeological studies in the choshuichi alluvial fan, Taiwan: Groundwater, **40**, 165–173.

Yeh, T.-C. J., S. Liu, R. J. Glass, K. Baker, J. R. Brainard, D. Alumbaugh, and D. LaBrecque, 2002, A geostatistically based inverse model for electrical resistivity surveys and its applications to vadose zone hydrology: Water Resources Research, **38**, 14–1.

Acknowledgments

CNPq is thanked for theresearch fellowship and associated grant (Proc. 304301/2011-6) for WEM. The used computers were acquired with financial support from the INCT-GP.